Prediction of Micro-crack Densities in Cryogenic IM7/977-2 Propellant Tanks

Xiaofeng Su and Frank Abdi
Alpha STAR Corporation, Long Beach, CA
and
J. Andre Lavoie
Northrop Grumman Corporation, CA

ABSTRACT

The micromechanics model, equivalent constraint model, was combined with the finite element analyzer GENOA to predict micro-crack density evolution and corresponding material degradation in polymer composite structures. As an example of predicting crack densities in cryogenic propellant tanks, an IM7/977-2 25-inch disk under assembly loading and pressure was simulated. The simulation gave micro-crack density distribution through the entire disk at various strain levels. Prediction was compared with the corresponding test results conducted at NASA. A coupon model under uni-axial tension was also given for demonstration of the method.

INTRODUCTION

Cryogenic polymer composite propellant tanks are widely employed in Reusable Space Vehicles due to their lightweight. However, leakage tends to occur when micro-damages exceed tolerable levels, which may cause catastrophic tank failure. Micro-cracks, formed in the polymer matrix during manufacturing and service, significantly contribute to the leakage of composite propellant tanks. Therefore, predicting micro-crack formation and development in cryogenic tanks is of great importance to tank design.

Methods for calculating stress fields in cracked laminates are the variational approach [1], the shear lag method [2] [3], approximate elasticity [4] and internal variable models [5]. The shear lag method is an efficient and simple means of calculating stresses in laminate fibers and matrix. It has also been extended to micro-crack density prediction in laminates. Zhang et al [6] [7] developed an equivalent constraint model (ECM), which predicts the reduction in stiffness properties due to transverse ply cracks as well as the initiation and growth of matrix cracking with increasing the mechanical load. In their study, an improved two dimensional (2-D) shear lag analysis was used to determine the stress distribution in the cracked laminates. Though crack density prediction using this method shows consistency with test results, it can only be applied to simple lay-ups subjected to uni-axial tension.

In order to predict micro-crack densities in structures, the equivalent constraint model was incorporated in a progressive failure finite element analyzer (GENOA) for this study. Stress and strain fields calculated using the finite element analyzer were transferred into the ECM. Within the ECM, the average stress and strain fields in each constituent were used to calculate the micro-crack formation and development described by the magnitudes of micro-crack density. This method assumed that the micro-crack spacing was uniform in the ECM. Only transverse cracking was considered in the ECM. For demonstration of the method, a coupon model was simulated under uni-axial tension and compared with corresponding test data [8]. As an example of predicting crack density in cryogenic propellant tanks, an IM7/977-2 25-inch disk under assembly loading and pressure was simulated. The simulation gave micro-crack density distribution through the entire disk at various strain levels. Prediction was compared with the corresponding test results conducted at NASA [9]. The probabilistic sensitivity analysis was also performed to understand the effects of material parameters on the crack density evolution in the pressured disk case.

Combination of the ECM with GENOA allows the unit cell model to be used at the structural level. It predicts the entire crack density profile through polymer composite structures. Thus, it is a powerful tool for the permeability and damage tolerance design of polymer composite cryogenic propellant tanks.

METHODOLOGY

The crack density prediction using the ECM gives the entire profile of crack density distributions through a structure during the loading process. At each location of the structure, the crack density is obtained at the ply level. Prediction of the crack density in laminate matrix in GENOA consists of,

1) The onset of cracks in matrix,
2) The multiplication of cracks in matrix, and
3) The degradation of composite properties due to the existence of cracks.

Figure 1 shows the procedure of the crack density calculation using GENOA.

Onset of Cracks in the Matrix - The onset of cracks in the matrix is predicted by the transverse tensile failure criterion. It occurs when

$$\sigma_{22} \geq \sigma_{22T} \tag{1}$$

In Equation 1, σ_{22} is the ply transverse tensile stress and σ_{22T} is the ply transverse tensile strength.

Multiplication of Cracks in the Matrix – The multiplication of matrix cracks is defined by the progressively increasing crack density and is predicted by the assumption that the energy released due to damage in the matrix forms new crack areas. Therefore, the crack density at each load level is derived based on the energy release rate equation, which is established by the damage energy release rate (*derr*) equal to the first partial derivative of the potential energy with respect to crack areas. At each load level,

$$derr = \alpha \frac{\partial (P - U)}{\partial (C_d \times A_e)} \tag{2}$$

where P is the external work done by the applied forces and U is the strain energy. C_d is the crack density and A_e is the cracked area. In finite element analysis, A_e is the damaged element area, and the partial derivative becomes the finite differential. α is a conversion factor relating *derr* to the strain energy release rate which is used instead of *derr* in Equation 2 in classical fracture mechanics. By this approach, we are able to calculate the crack density from the material strength and modulus instead of the fracture toughness. The definition of *derr* is

$$derr = \frac{1}{2V_d} \int_{V_d} \sigma_m^2 \times (1 - v_f) \times D / E_m dv \tag{3}$$

where σ_m and E_m are the matrix strength and modulus, respectively. v_f is the fiber volume fraction. D is the damage factor of the matrix adopted as the degradation factor of the lamina stiffness in the transverse direction (Λ_{22} in Equation 6). V_d is the damage volume that is computed from

$$V_d = A_e \times t \tag{4}$$

t is the laminate thickness.

The crack density C_d can be obtained by combining Equations 2 and 3.

Degradation of Composite Properties due to the Existence of Cracks - The degradation of composite properties due to the existence of cracks is calculated by the Equivalent Constraint Model developed by Zhang et al [6, 7]. An iterative process was introduced in the GENOA/ECM model to consider stress redistribution resulted from the damage in the matrix. In each iteration, the crack densities and the corresponding degradations of composite properties are re-calculated. The iteration reaches convergence when crack densities through the structure reach saturation under the current load level. New cracks may occur when the load moves to the next level.

The degraded lamina stiffness can be written as follows:

$$\begin{bmatrix} Q_{11}^d & Q_{12}^d & 0 \\ Q_{12}^d & Q_{22}^d & 0 \\ 0 & 0 & Q_{66}^d \end{bmatrix} = \begin{bmatrix} Q_{11}^o & Q_{12}^o & 0 \\ Q_{12}^o & Q_{22}^o & 0 \\ 0 & 0 & Q_{66}^o \end{bmatrix} - \begin{bmatrix} Q_{12}^{o^2} / Q_{22}^o \times \Lambda_{22} & Q_{12}^o \times \Lambda_{22} & 0 \\ Q_{12}^o \times \Lambda_{22} & Q_{22}^o \times \Lambda_{22} & 0 \\ 0 & 0 & Q_{66}^o \times \Lambda_{66} \end{bmatrix} \tag{5}$$

where Q_{ij}^o and Q_{ij}^d are original and degraded stiffness, respectively. The subscripts 1 and 2 represent, respectively, the ply longitudinal (fiber) and transverse directions. Λ_{22} and Λ_{66} are degradation factors, defined in the following equations

$$\Lambda_{22} = 1 - \frac{\phi_1 + \phi_2 C_d \tan(\lambda_1 / C_d)}{\phi_1 + \phi_3 C_d \tan(\lambda_1 / C_d)} \tag{6}$$

$$\Lambda_{66} = 1 - \frac{\Gamma_1 + \Gamma_2 C_d \tan(\lambda_2 / C_d)}{\Gamma_1 + \Gamma_3 C_d \tan(\lambda_2 / C_d)} \tag{7}$$

The parameters ϕ_1, ϕ_2, ϕ_3, λ_1, Γ_1, Γ_2, Γ_3, and λ_2 are related to lamina properties and laminate ply schedules. Their expressions are in References 6 and 7. The ply degradation factors, Λ_{22} and Λ_{66}, concern not only the properties of the current ply but also those of other plies in the laminate. Therefore, the constraining effect of adjacent plies is considered in the formation of ply degradation factors.

RESULTS

Predictions of crack densities were performed to the coupon under uni-axial tension and the 25-inch diameter disk under pressure. Degradation of laminate stiffness due to micro cracking was computed. The probabilistic sensitivity analysis was also performed to understand the effects of material parameters on the crack density evolution in the pressured disk case.

Material Properties – The material of the coupon is IM600/Q1334. The material system of the 25-inch diameter disk is IM7/977-2 (Rockwell 1995 data [10] was used since we didn't have the material data in the NASA test [9]).

IM600: E_{11} = 34.5msi, S_{f11T} = 560 ksi.
Q1334: E_m = 0.9 msi, S_m = 14 ksi, v = 0.34.

IM7: E_{11} = 40 msi, S_{f11T} = 660 ksi.
977-2: E_m = 1.6 msi, S_m = 9.9 ksi, v = 0.48

Finite Element Models – The coupon and disk models are illustrated in Figures 2a and 2b. The coupon model is 20"x5" and consists of 100 shell elements. The tension load was applied at the longitudinal direction. Two laminate configurations, $[45/-45/90_2]s$ and $[0_2/-60_2/60_2]s$, were considered in simulation.

Only a quadrant model of the disk was utilized in simulation. The symmetrical boundary conditions were applied to the cut edges. Both assembly and pressure loads were considered (Figure 2b). The quasi-isotropic laminate configuration is $[0/45/90/-45]_s$

Tension of The IM600/Q1334 Coupon - The profiles of the crack density development were obtained during the entire load processes. The crack densities in 90-degree plies of $[45/-45/90_2]s$ and 60-degree plies in $[0_2/-60_2/60_2]s$ were compared with test data [8] in Figure 3. The simulation results are consistent with the test data.

25-Inch Disk under Pressure – The micro crack development was predicted at various strain levels in the disk. The corresponding laminate stiffness degradation was also calculated. At the end, a probabilistic sensitivity analysis was conducted to understand the effect of each material parameter on the micro crack formation and development.

Figures 4a to 4c illustrate the distribution of the micro crack density in the outer layer at various strains. The pressure-applied layer is defined as the inner layer. The strains were measured on the central inner layer.

Simulation shows cracks were formed in the disk center, and then propagated outward to the disk edge. Another source of cracks is locations 10" to the disk edge due to the stress concentration caused by the assembly clamps.

Degradation of the laminate stiffness at various strain levels is shown in Figures 5a to 5c. The degradation was measured at four locations from the disk center to the edge. At the strain level of 5790 (micro in/in), the laminate tensile and shear moduli dropped about 10% while the Poisson's Ratio increased by 8.8%.

The simulation was compared with the test data [9] at four locations starting from the disk center to the edge in Figure 6. The strain at the top ply of the disk center is 4800 micro strains. The crack density shown is in the outer ply. The test shows the crack density at the disk center is almost twice of the simulation. Except this, the numerical results reasonably agree with the test data.

The sensitivity of the crack density development to the material properties is shown in Figure 7. The strain level at the mean value is 4850 micro strains. The material properties were varied by 10% in the probabilistic sensitivity analysis. All the data for eight plies is shown. It can be seen that the most effective parameters are the fiber modulus, matrix strength and fiber volume fraction. This is because increasing fiber modulus and volume fraction reduces the stress in matrix, and increasing the matrix strength increases the matrix load-carrying ability. Both reduce the micro crack level in matrix.

CONCLUSIONS

1. Higher strains usually cause more micro cracks. Therefore, the disk center has more cracks than other areas.
2. Laminate stiffness degrades due to existence of micro-cracks. Degradation levels of laminate tensile and shear moduli as well as Poisson's Ratios are similar.
3. To reduce the crack densities, the fiber longitudinal modulus, fiber volume fraction and matrix strength should be increased, while the matrix modulus and fiber transverse modulus should be decreased.
4. Combination of the ECM with GENOA allows the unit cell model to be used at the structural

level. The simulation results agree with test data reasonably well.

REFERENCE

1. HASHIN, Z., "Analysis of Cracked Laminates: A Variational Approach," *Mech. Mater*., Vol. 4 pp121-136, 1985.
2. Laws, N. and Dvorak, G.J., "Progressive Transverse Cracking in Composite Laminates," *J. Comp. Mater.*, Vol. 22, 1988.
3. Han, Y.M. and Hahn, H. T., "Ply Cracking and Property Degradations of Symmetric Balanced laminates under General In-plane Loading," *Composite Sci. Tech.*, Vol. 31, pp 165-177, 1989.
4. Nuismer, R.J. and Tan S.C., "Constitutive Relations of A Cracked Composite Lamina," *J. Composite Mater*., Vol. 22 , pp 306-321, 1988.
5. Allen, D.H. and Harris, C.E,, "A Thermomechanical Constitutive Theory for Elastic Composites with Distributed Damage," *Int. J. Solids Strut.*, Vol. 23, pp 1301-1308, 1987.
6. Zhang, J., Fan, J. and Soutis, C., "Analysis of Multiple Matrix Cracking in [±θm/90n]s Composite Laminates – Part 1: In-plane Stiffness Properties," *Composites*, Vol. 23, No. 5, 1992.
7. Zhang, J., Fan, J. and Soutis, C., "Analysis of Multiple Matrix Cracking in [±θm/90n]s Composite Laminates – Part 2: Development of Transverse Ply Cracks," *Composites*, Vol. 23, No. 5, 1992.
8. Tomohiro, Y., Takahira, A. and Takashi, I., "Transverse Cracking in CFRP Laminates with Angled Plies," *43rd AIAA Structures, Structural Dynamics, and Materials Conference*, Denver, Co, AIAA-2002-1255, April 2002
9. Bohlen, J.W., Sheu, C., Dyer T. and Palm, T., "Composite Cryotank Material Properties", *RLV/SOV Airframe Technology Conference*, Nov. 19-22, 2002.
10 Greenberg, H.S., " Milestone 10-Test Report of Composite Tank Material Screening Tests Rockwell Aerospace Report", May 5, 1995.

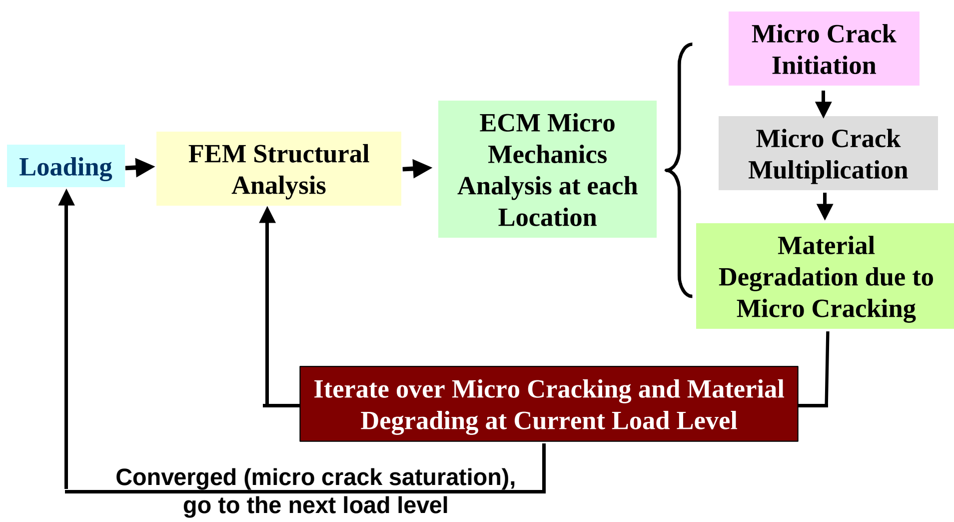

Figure 1 Procedure of the crack density calculation using GENOA

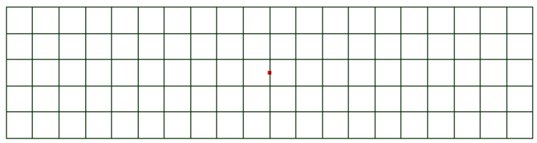

2 (a) The finite element model of the coupon.

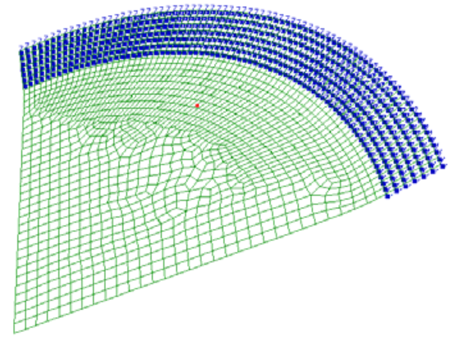

2 (b) The quadrant model of the 25-inch diameter disk. The blue area was clamped to simulate the assembly load. The enforced displacement at the edge is 0.3188”. The rest area is under pressure loading

Figure 2 Finite element models of the coupon and disk

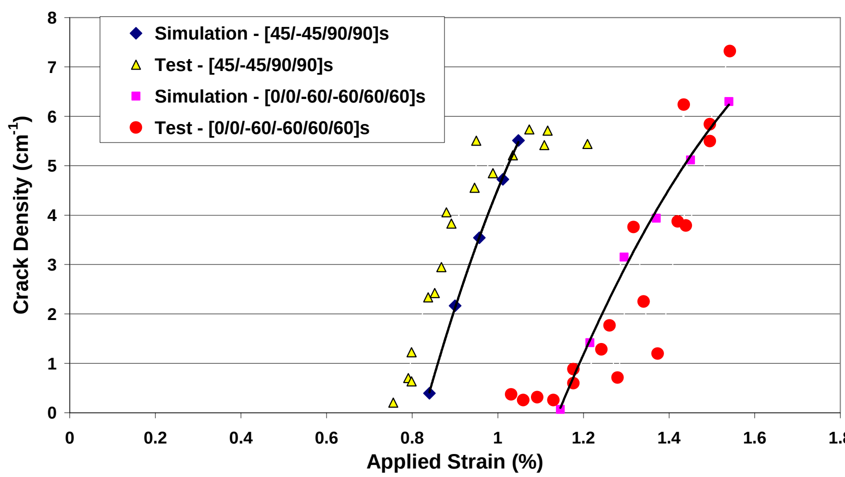

Figure 3 Comparison between the simulated crack densities and test data [8] in 90-degree plies of [45/-45/90$_2$]s and 60-degree plies in [0$_2$/-60$_2$/60$_2$]s]

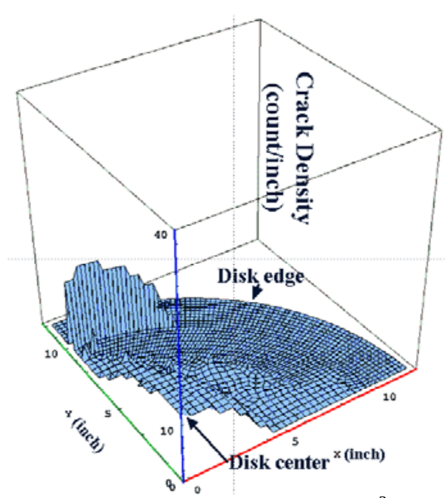

4 (a) Strain = 4.15x10^{-3}

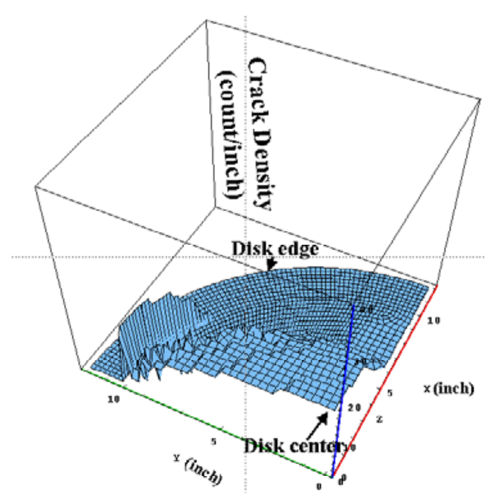

4 (b) Strain = 4.76x10^{-3}

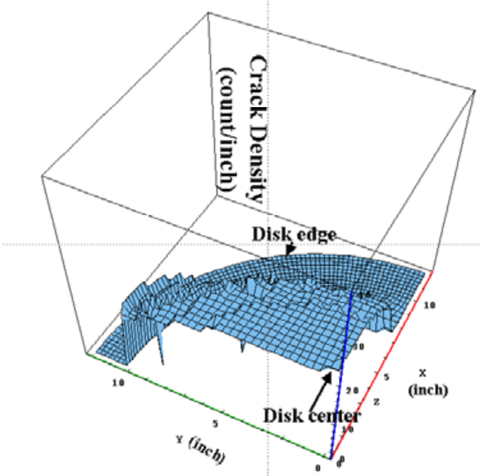

4 (c) Strain = $5.8x10^{-3}$

Figure 4 Distribution of the micro crack density in the outer layer of the disk at various strains.

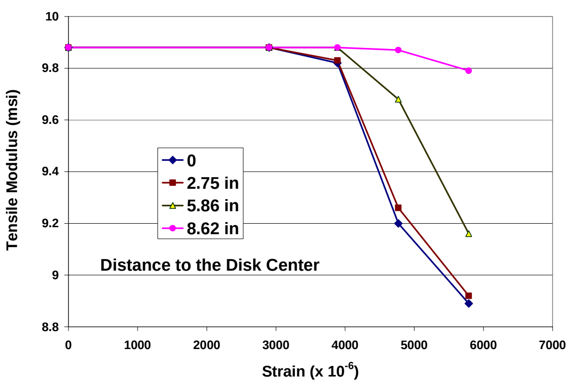

(a) Laminate tensile modulus

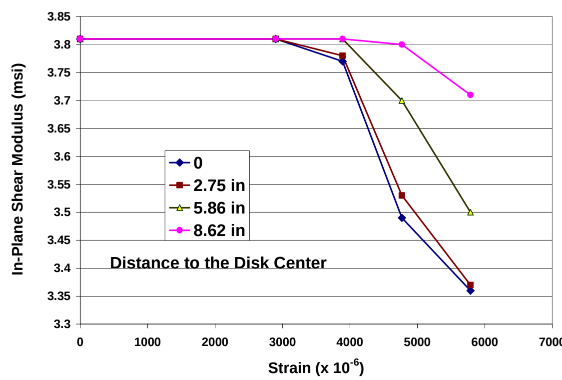

(b) Laminate in-plane shear modulus

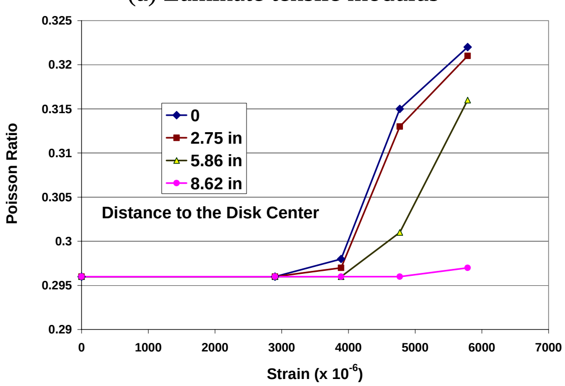

(c) Laminate Poisson ratio

Figure 5 Degradation of the laminate stiffness of the disk at various strain levels

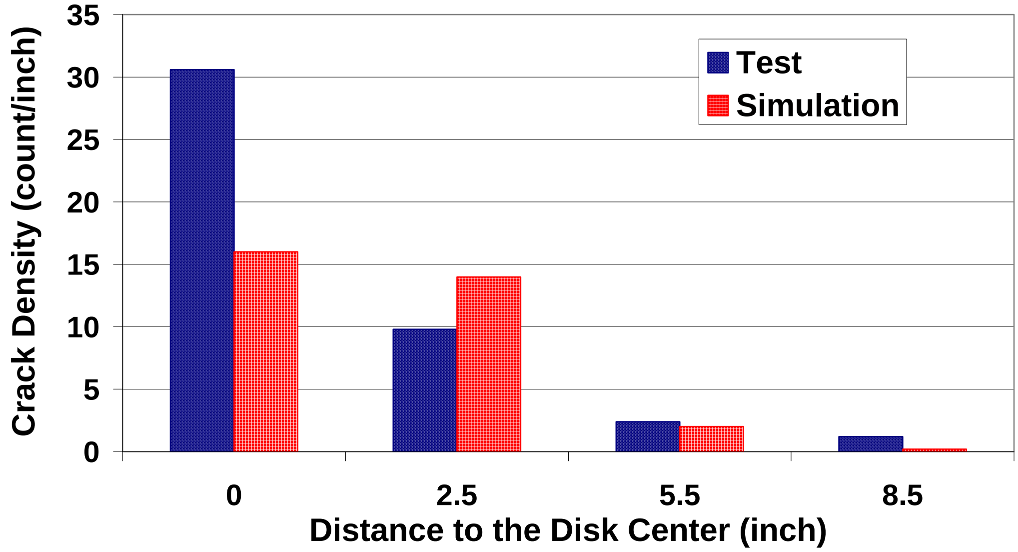

Figure 6 Comparison between the simulated crack density and the test data [9] in the disk. The strain at the top ply of the disk center is 4800 micro strains

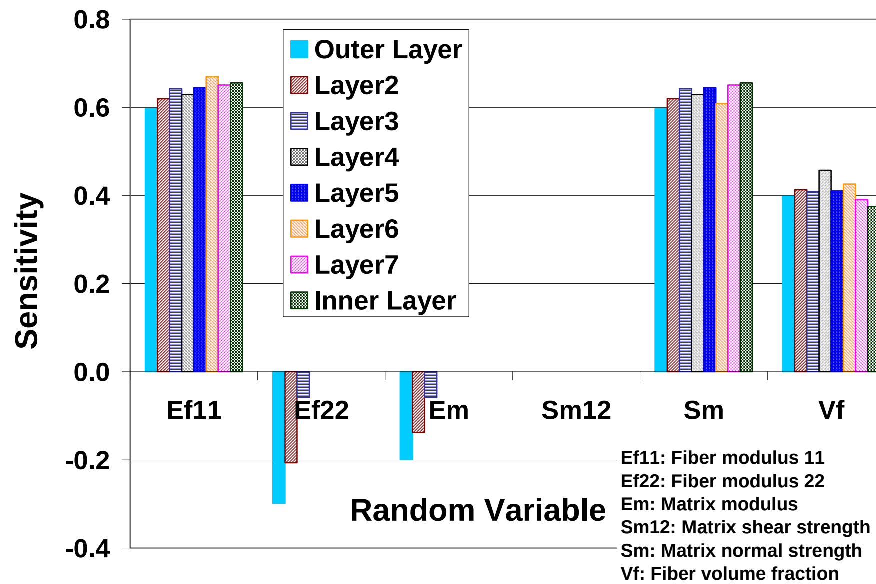

Figure 7 Sensitivity of the crack density development to the material properties in the disk